Herschel PACS ICC

On the comparison of PACS 160 μm maps and AKARI 140 μm maps

Document Ref.: PICC-CR-TN-047

Issue: 1.0

Prepared by: Stefano Pezzuto
Luca Calzoletti

Date: December 14, 2015

Document Status Sheet

Document Title: On the comparison of the PACS 160 μm maps with the AKARI 140 μm maps			
Issue	**Revision**	**Date**	**Reason for change**
1	0	December 14, 2015	First version

Contents

1 Purpose of this document

The zero-level of the diffuse emission in the instruments PACS and SPIRE is not known: assuming that the two instruments are well calibrated, for maps of a few square degrees the only correction to apply is a constant (offset) to be added algebrically to each point of the map. For the SPIRE instrument, the overlap between its photometric bands and the Planck bands makes it possible to derive such an offset by a, more or less, direct comparison of the emission as measured by the two instruments. This is quite a safe correction and a general procedure to derive it has been already implemented in HIPE. For PACS, estimating the correction is not trivial because its bands are at frequencies higher than those observed with Planck; nonetheless, by using the IRAS all-sky survey, it is possible to compute an IRAS-Planck correction (Bernard et al. 2010): the spectral energy distribution (SED) at a given position is constructed from the IRAS and Planck data, and from this SED the expected value at 160 μm is derived. This work is applied to all the pixels of the map to obtain an average coefficient.

The aim of this note is to investigate the possibility to use AKARI observations to find the PACS 160 μm coefficient: AKARI WIDE-L band has an effective wavelength of 140 μm (Takita et al. 2015, hereinafter AkaPaper), much closer to the PACS red band than IRAS 100 μm filter. AKARI has been calibrated against COBE/DIRBE data sets with an accuracy which is estimated better than 10% for $I_\nu > 25$ MJy/sr (AkaPaper). In principle, it could be possible to adopt the same approach to derive the zero-level coefficients for the PACS 70 μm and 100 μm bands by a comparison with the AKARI N60 and WIDE-S bands centred at 65 μm and 90 μm: this possibility is not investigated in this document, but it may be feasible.

The result of this note, for the general user, is a recipe to follow to calibrate her/his own PACS photometry observations: given the short time available before the end of the PACS ICC operations it is not possible to make an extensive test of the procedure, nor to derive its reliability ot its applicability to the hundreds of maps obtained with PACS. It will be up to the user to estimate, somehow, the quality of the result for a generic case.

2 The comparison between PACS and AKARI data

The procedure here described to derive the zero-level coefficient, or offset, can be applied to any PACS 160 μm map, indipendent on its size, or observing mode. It should be noted, however, that it seems more appropriate to calibrate separately two or more maps before combining them in a mosaic, rather than to create first a large mosaic out of many fields and afterward to look for one single offset.

Once the map to calibrate[1] is available (in this note we will make use of maps obtained in different ways) the first step is to download from internet the corresponding AKARI map. The whole data set can be queried here: `http://www.ir.isas.jaxa.jp/AKARI/Archive/Images/FISMAP/`. For a given spatial field, four maps are available for the four bands: in this note we will consider the WIDE-L observations.

The PACS map needs to be degraded to the AKARI resolution (88″, see AkaPaper). We used a slightly modified version of the script `PhotometryConvolveResolutionKernel.py` available in HIPE.

The PACS map so obtained has then to be compared with the AKARI one: a plot I_ν(PACS) vs. I_ν(AKARI) should be a straight line of the form $y = mx$ with $m = 1$ for two identical photometry systems. The fact that $y(x = 0) \neq 0$ shows that there is an offset between the two maps. In principle one can plot Herschel fluxes vs. AKARI fluxes to derive the offset without any knowledge of the two instruments, but as we shall see this is not possible because the AKARI fluxes do not reach the zero level (and in any case it is better to consider $I_\nu > 25$ MJy/sr, as said). We need then to go through m and this parameter depends on the differences between the two instruments bands and on the source spectrum.

2.1 The transport of flux between the two bands

Given a SED $f_\nu(\lambda)$ we want to compare the flux measured with two different instruments: the comparison requires to "transport" one photometric system to the other[2].

[1] We will make use of the verb "to calibrate" for simplicity given the fact that the PACS maps *are* indeed calibrated.

[2] Note that in principle this procedure may be necessary also if the measurement is done at the same wavelength.

Table 1: Color corrections for two models and three temperatures.

T	$B(T)$		$\nu^{-2}B(T)$	
	Akari	Ours	Akari	Ours
10	1.549	1.552	2.048	2.052
50	0.937	0.937	1.003	1.003
3000	0.937	0.937	0.964	0.964

Table 2: The factors in Equation (2) for different T (in K) and β=2. At low temperatures, T <10 K, the values are quite uncertaint.

T		T		T		T		T	
5	3.6823	15	1.1574	25	0.9494	35	0.8771	45	0.8416
6	2.7124	16	1.1211	26	0.9391	36	0.8725	46	0.8391
7	2.1881	17	1.0903	27	0.9297	37	0.8682	47	0.8366
8	1.8691	18	1.0639	28	0.9211	38	0.8641	48	0.8343
9	1.6585	19	1.0410	29	0.9132	39	0.8603	49	0.8321
10	1.5107	20	1.0209	30	0.9060	40	0.8567	50	0.8300
11	1.4020	21	1.0032	31	0.8993	41	0.8533	100	0.7840
12	1.3189	22	0.9875	32	0.8931	42	0.8502	500	0.7550
13	1.2535	23	0.9734	33	0.8874	43	0.8472	1000	0.7519
14	1.2008	24	0.9608	34	0.8821	44	0.8443	5000	0.7495

Let us start by naming F_4 and F_6 the flux measured by AKARI at 140 μm and by PACS at 160 μm, respectively. We have

$$F_{\nu_4} = \frac{\int f_\nu(\nu) T_4(\nu) \mathrm{d}\nu}{\Delta\nu_4} \tag{1}$$

where $T_4(\nu)$ represents the function that describes the spectral response of the optics (including also the response of the detectors); for the PACS band a similar equation holds with $T_6(\nu)$.

In a previous technical note (Pezzuto 2013) it has been shown how $\Delta\nu$ can be derived for the PACS bands: $\Delta\nu_6$=30.2 μm[3]. The same computation for the WIDE-L band of AKARI has been made by using the optics response available at `https://www.ir.isas.jaxa.jp/AKARI/Observation/support/FIS/RSRF/FIS_RSRF_070122.txt`: the result is $\Delta\nu_4$=51.9 μm, in perfect agreement with the value of 52.4 μm reported by the team instrument (Kawada et al. 2007). In Table 1 the color corrections are compared, those found by us with those given by the instrument team in a few cases: the agreement is excellent. In the following we adopted the values we have derived.

It is straightforward to write

$$F_{\nu_6} = \frac{\Delta\nu_4}{\Delta\nu_6} \frac{\int f_\nu(\nu) T_6(\nu) \mathrm{d}\nu}{\int f_\nu(\nu) T_4(\nu) \mathrm{d}\nu} F_{\nu_4} \tag{2}$$

The dust emission at the far-infrared wavelengths is well described with a modified blackbody function

$$F_\nu \propto \nu^\beta \mathrm{B}_\nu(T) \tag{3}$$

where $B_\nu(T)$ is the Planck function and β is the dust emissivity (or opacity) index. In the following we set β=2 because this is one of the most common values used in literature: without data at long wavelengths, from (sub)mm onward, it is not possible to costraint β and, in any case, it is known that β varies within the same region. But, on the average, the value 2 is a good choice for Herschel data (see Sadavoy et al. 2013 for a detailed discussion). With this choice, the integral term in Equation (2) depends only on the temperature T. In Table 2 the proportionality factors for β=2 are reported for a set of T.

[3]We use indifferently in the same formula wavelengths and frequencies; only when dν or dλ are involved it makes a difference.

Table 3: Test of Equation (2): T, temperature in K; F_{160}, monocromatic flux (Jy) at 160 μm; P/A, ratio between monocromatic flux at 160 μm and in-band flux at 140 μm; F_{140} expected flux (Jy) in the WIDE-L band; $F_{\rm A}$, measured flux (Jy); σ, difference between fifth and sixth columns in unit of standard deviations. An exponent [1] after the name of the star means that the quality flag for that source is 1, i.e. the source is not confirmed. Data of second and third columns from Baltog et al. (2014).

Name	T	F_{160}	P/A	F_{140}	$F_{\rm A}$	σ
β And	3880	1.062	0.8183	1.30	1.71±0.34	1.2
α Cet[1]	3740	0.928	0.8184	1.13	0.54	
α Tau	3850	2.677	0.8183	3.27	3.48±0.83	0.3
α Boo	4320	2.891	0.8182	3.53	4.13±0.34	1.8
γ Dra[1]	3960	0.621	0.8183	0.759	1.46±0.58	1.2

To test Equation (2) we used the set of stellar calibrators used for PACS, transporting the expected flux at 160 μm in the AKARI band and comparing the value with the measurement in the AKARI FIS point sources catalogue (`http://darts.isas.jaxa.jp/astro/akari/cas/tools/search/radial.html`). The results of the comparison are in Table 3: we see that the flux transported to the 140 μm band agrees within $\sim 1\sigma$ for almost all the values, with α Boo at $<2\sigma$. The measured flux of α Ceti may be wrong.

2.2 The Planck temperature map

As we shall see, we need a knowledge of the dust temperature to derive the offset. To this aim we used the Planck dust temperature (Planck 2014) available at this address: `http://irsa.ipac.caltech.edu/data/Planck/release_1/all-sky-maps/previews/HFI_CompMap_ThermalDustModel_2048_R1.20/index.html`. The temperature map for a specific sky region has been extracted using the *healpix* utilities in IDL.

2.3 The column density maps

The check on the accuracy of the offset found is made after the column density map is derived: to this aim the PACS 160 μm map and the SPIRE 250 μm and 350 μm maps are degraded to the SPIRE 500 μm resolution and projected on the same WCS grid (the same HIPE script as before has been used, with the available on-line kernels). Then, pixel by pixel, the following function is fit

$$I_\nu = 0.1 \left(\frac{300}{\lambda}\right)^2 2.8 m_{\rm H} N_{\rm H_2} {\rm B}_\nu(T) \qquad (4)$$

where I_ν is the measured flux density in MJy/sr in the 4 bands; λ is in μm; $m_{\rm H}$ is the mass of the atom of hydrogen in grams; $N_{\rm H_2}$ is the column density of molecular hydrogen in cm^{-2}; ${\rm B}_\nu(T)$ is the Planck function also in MJy/sr. For a justification of this formula see, e.g., Könives et al. (2015).

The two free parameters are T and $N_{\rm H_2}$: the fitting procedure is based on that used in Pezzuto et al. (2012), i.e., a grid of models at the temperatures $T \leq 50$ K shown in Table 2 is computed and for each T the best value of the column density is computed; finally, the model giving the smallest residual is selected as best. The procedure is written in C and can be run with or without computing the color corrections for the Herschel bands. For this note the grid of models has been computed without color corrections. For an area of $\sim$30 deg^2 the time to run the code is about 15 minutes or less. The output of the code is: the map of column density; the map of the dust temperature; the uncertainties on the column density. To follow the Gould Belt Survey consortium, an uncertainty of 20% has been assigned to the PACS band, and of 10% to the SPIRE bands.

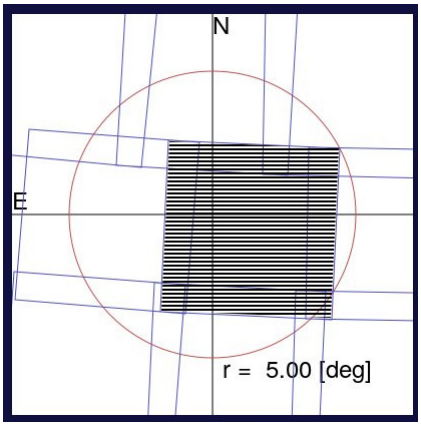

Figure 3-1: The overlap between AKARI fields and a circular region of radius 5 degrees centred on the Aquila star-forming region observed with Herschel. The dashed area is the selected field.

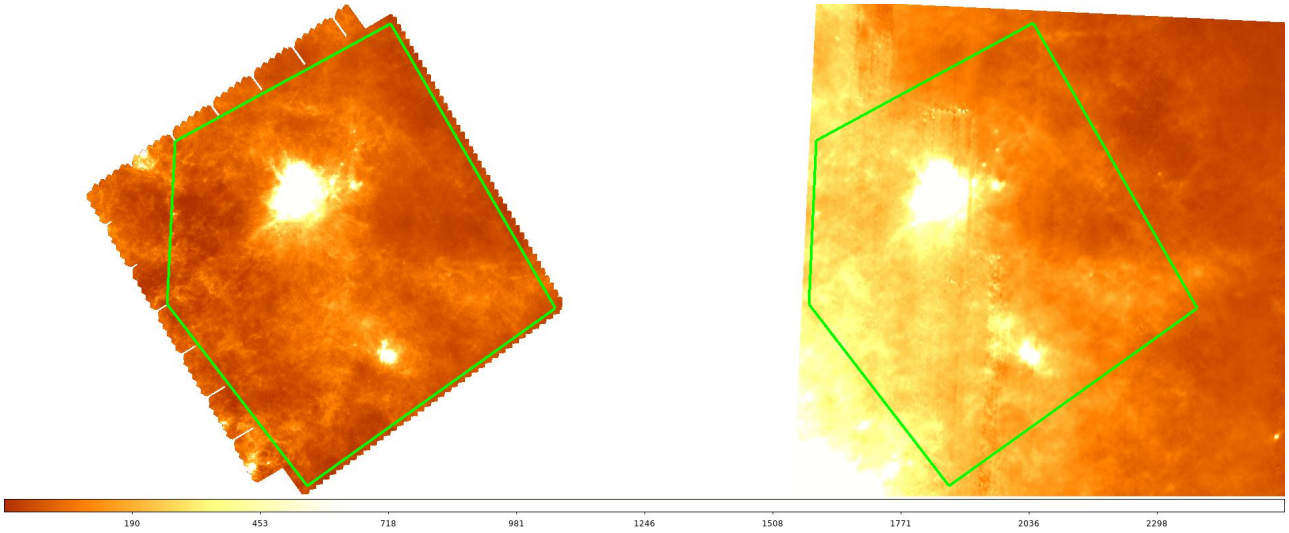

Figure 3-2: Left: the PACS field at 160 μm of the Aquila region (from the GBS consortium); right: the (276.69,+20.00) field observed with AKARI at 140 μm. The two fields have been projected on the same WCS (AKARI delivers the maps in ecliptic coordinates) and on the same scale (in MJy/sr). The green line encloses the area common to the two fields used for the comparison.

3 Three test cases

3.1 The Aquila region

The star-forming region in Aquila is located at about 260 pc. It has been observed in parallel mode (OBSID 1342186277 and 1342186278) during the Science Demonstration Phase as representative target of the Gould Belt Survey (GBS) KP. A full analysis of these observations has been published by Könyves et al. (2015). As products associated to the paper, the maps, which we used, have been made available on the GBS web site, see `http://www.herschel.fr/cea/gouldbelt/en/Phocea/Vie_des_labos/Ast/ast_visu.php?id_ast=66`. The maps offsets have been computed according to the usual scheme based on Planck data (Bernard et al. 2010). These offsets are written in the FITS header of the maps and have to be added to the intensity, which has been done for the SPIRE bands.

The AKARI web site has been queried using the centre coordinates of the column density map obtained by the GBS consortium, also available on their site (HGBS_aquilaM2_column_density_map.fits.gz); and using a search radius of 5 degrees. The result of the query is shown in Figure 3-1.

The overlap of the Herschel field and the AKARI fields is not simple but one of the four fields, centred at ecliptic coordinates (276.69,+20.00), covers almost all the PACS region, as shown in Figure 3-2.

As written previously, the PACS map has been smoothed to the AKARI resolution using a Gaussian of FWHM $\sqrt{(88'')^2 - (11.''3)^2}$: note that the beam assumed by the GBS consortium, 13.″5 is slightly larger

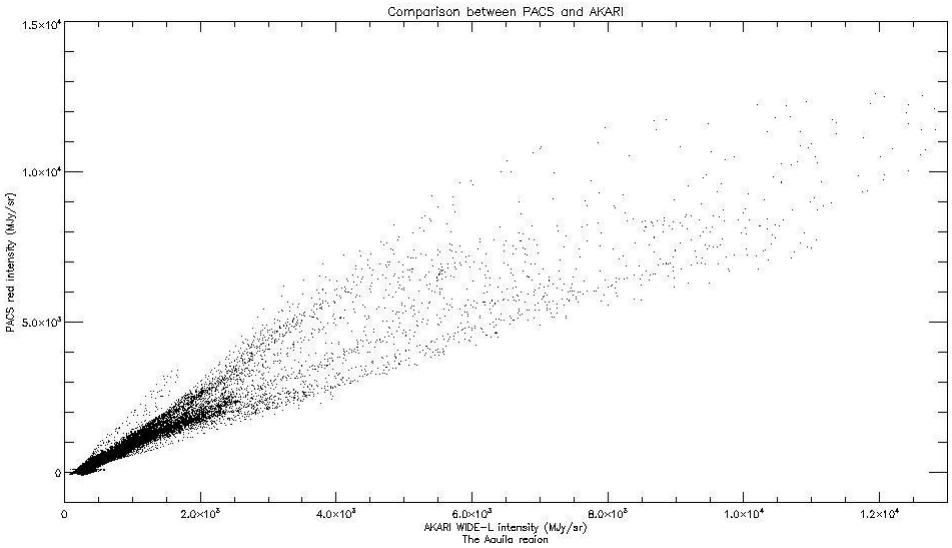

Figure 3-3: Pixel by pixel comparison of the intensities in the WIDE-L 140 μm band and in the PACS red 160 μm band.

than the beam hard-coded in the HIPE script, but for the purpose of this note this difference is considered not relevant. After the convolution the PACS map has been regridded with the IDL routine `hastrom` using the (celestial) WCS of the AKARI field. In Figure 3-3 the fluxes comparison is shown. It is clear that we can not fit the points distribution in the figure with a simple line $y = o + mx$ because we do not have all the points at the same temperature.

The method we pursuit is the following: for each spatial pixel (x, y) of the PACS map we found the dust temperature measured by Planck (clearly there is a correspondence many-to-one due to the different resolution). The slope m for that T has been found by interpolation of the values reported in Table 2; then, the corresponding offset is simply $o = mf_{\rm A} - f_{\rm P}$. The distribution of the offsets is shown in Figure 3-4. The peak of the distribution, 158 MJy/sr, agrees very well with the Planck-derived offset of 159.9 MJy/sr (Könives et al. 2015). There is then no need to make further comparisons.

3.2 The Perseus region

The Perseus molecular cloud is located at approximately 240 pc. It has been observed twice in parallel mode covering the West region (NGC 1333, B1, L 1448, L 1455) and the East region (IC 348, B 5) with a certain degree of overlap. A full analysis of this region, like the one performed for Aquila, is under preparation by the GBS consortium.

The PACS maps have been generated, on a common WCS which embraces the whole region, with Unimap (Piazzo et al. 2015); the data have been calibrated with the calTree version 45, according to the GBS convention. In Figure 3-5 the two fields are shown separately: the East part (left panel) and the West part (right panel): if we neglect a small portion of the East part, the whole field can be covered with three AKARI tiles. In Figure 3-6 a mosaic of the WIDE-L images, in the zone where they overlap with PACS data, is shown: this mosaic is only for graphical purposes and has not been used for analysis.

The search of the offset has been done as in the Aquila case: for the western part the offsets have been derived after comparing the PACS map with the three AKARI fields, one by one. The three resulting sets have been joint and the resulting distributionis shown in the right panel of Figure 3-7. The distribution for the eastern part is shown in the left panel of the same figure, where only the two tiles at ℓ 59.53 and 60.93 degrees have been used.

These figures are different from the previous case for two features: there are two peaks instead of one (even if another secondary peak is apparent in Figure 3-4) and the distributions are concentrated around the peaks instead of having a large, broad tail estending over a large range of offsets. The offsets found with Planck

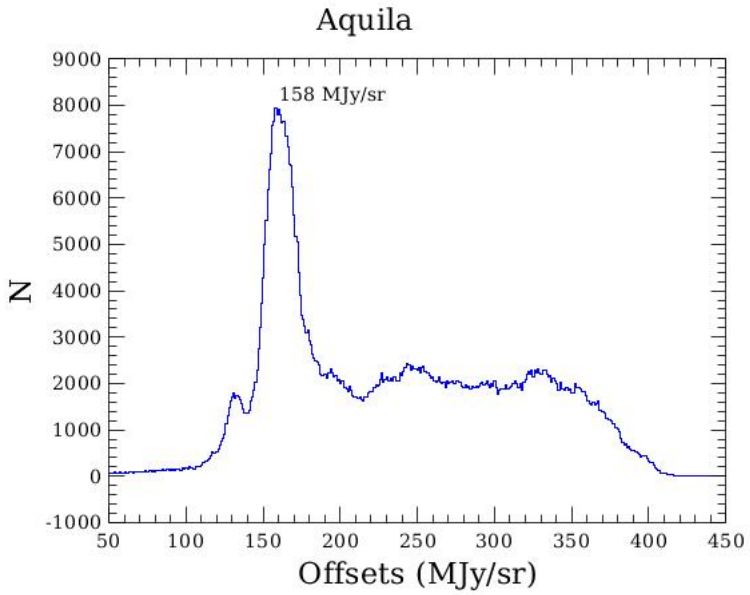

Figure 3-4: The distribution of offsets for each pixel common to the AKARI and PACS fiels.

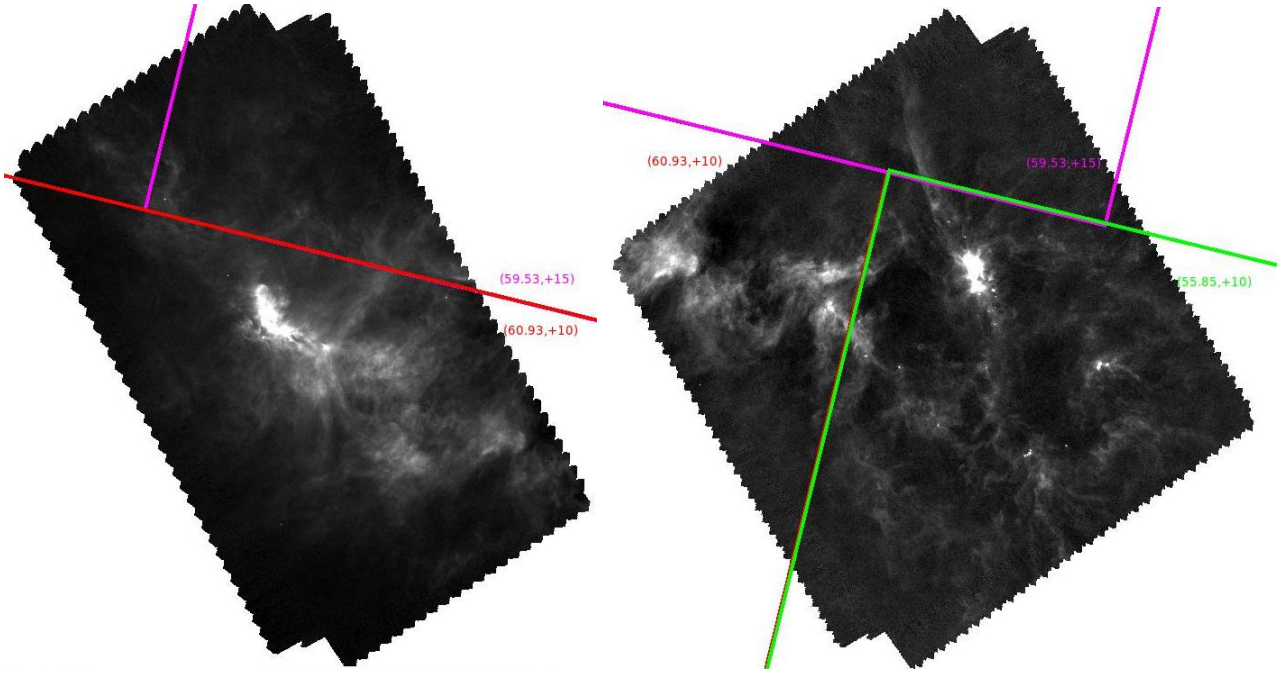

Figure 3-5: Left: East Perseus as observed with PACS at 160 μm; right: the West part. Three AKARI tiles, shown with the coloured boxes, are required to have a good coverage of the two PACS fields. PACS maps produced with Unimap.

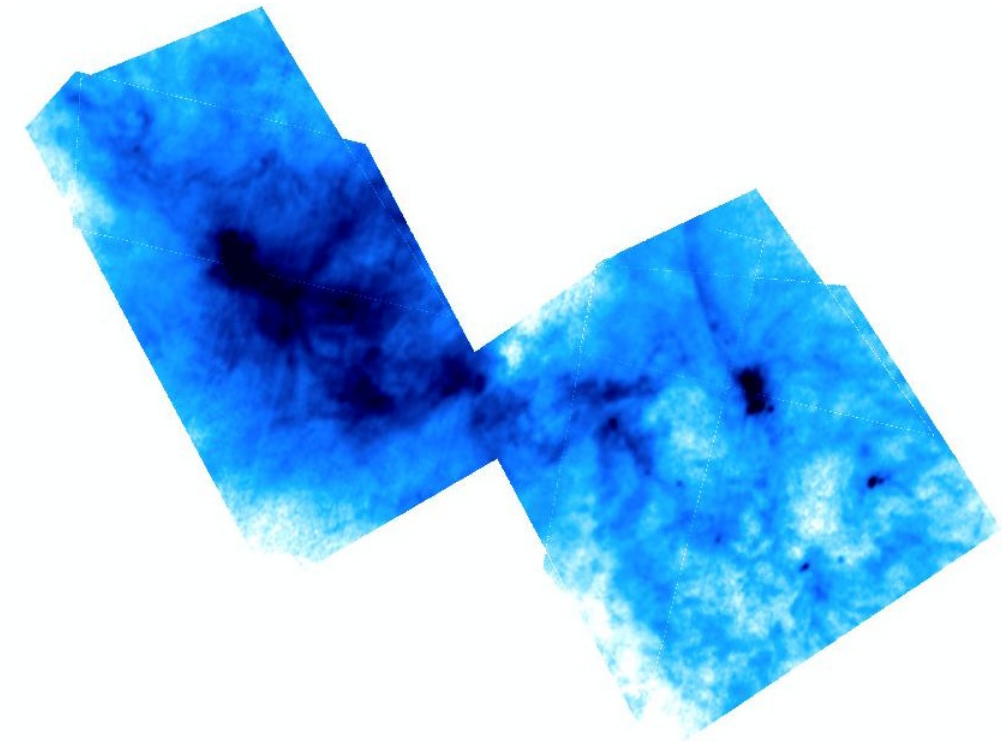

Figure 3-6: The three AKARI images combined in one region where they overlap with PACS data. In the common zones the tiles have been simply averaged: the resulting mosaic is shown to give a sketch of the region, for the analysis the three tiles have been used separately.

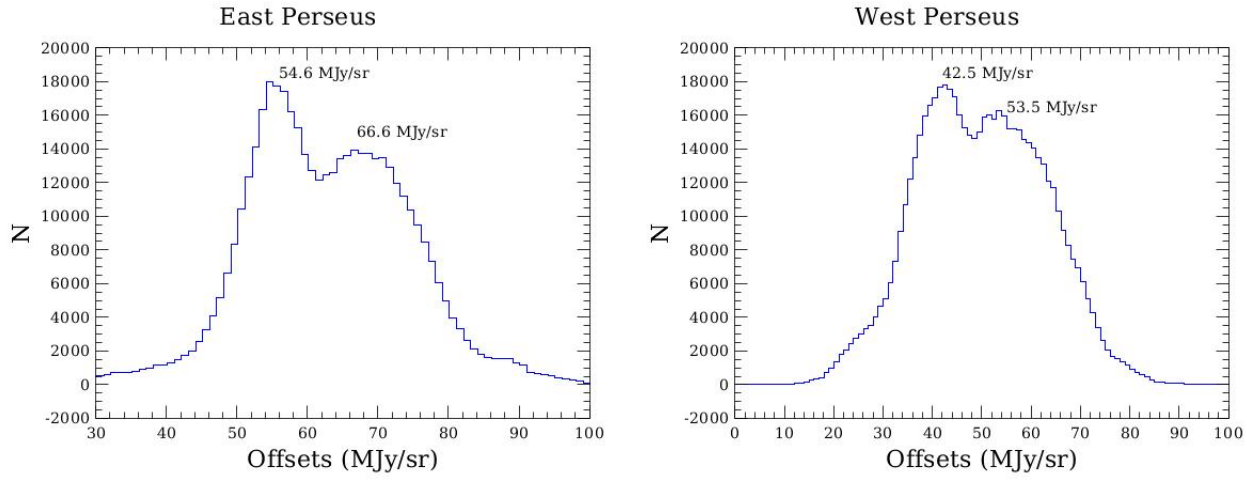

Figure 3-7: The distribution of offsets for the two Perseus fields.

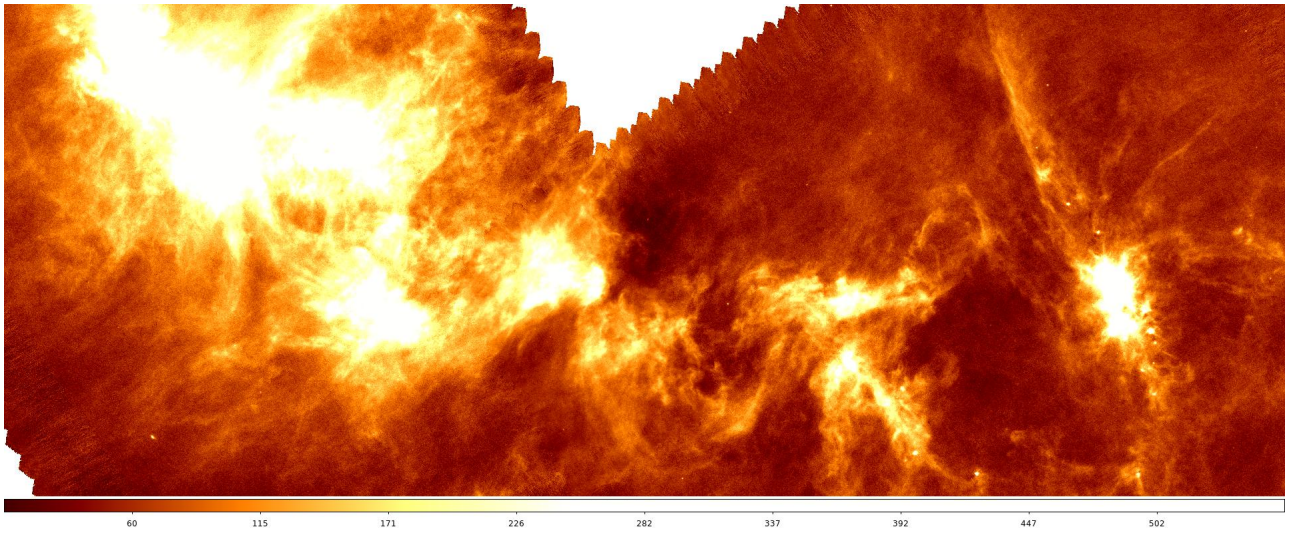

Figure 3-8: An enlargment of the PACS field after mosaicing the two images, corresponding to the overlapping region. The two fields match well each other, with only an artifact due to the turn-around zones, mainly of the West part.

$A_{\rm V}$	%
2	9.6
3	7.9
4	6.7
5	5.9
6	5.4
7	5.0
8	4.5
9	4.4
10	4.0

Table 4: For a given $A(\mathrm{V}_i)$ in mag, the mass enclosed within the $A(\mathrm{V}) > A(\mathrm{V}_i)$ contour is evaluated. This table reports the differences in percentage between the masses evaluated on the Planck-based map and on the AKARI-based map.

data are 76.4 MJy/sr and 54.6 MJy/sr for East and West Perseus, respectively, values that are very close the secondary peaks of both figures. A priori, however, we do not have any reason to choose one of the other peak, given the fact that they are comparable. For this reason we just computed the means (60.6 MJy/sr and 48.0 MJy/sr) and used these as offsets. They difference is 21% and 12% with respect to the Planck coefficients, a difference that requires some further comparison to be sure that our calibration is scientifically equivalent to the Planck calibration[4].

First we summed the two images after the different offset has been added: as said, the two PACS fields have been generated with Unimap imposing the same WCS, so there is a one-to-one correspondence between the spatial pixels in the two maps. In the overlapping region the intensity has been found simply by averaging the values of the two maps. A portion of the mosaic is in Figure 3-8 showing (part of) the overlapping region: there is no sign of a "step" effect which is visible when the two "calibrated" maps do not match well, i.e. when the two offsets are not compatible each other. Visible is only the pattern due to the turn-around zones of the maps, an effect that can be easily removed with a mask but that is not relevant for this work.

This map has been degraded to the SPIRE 500 μm resolution and used with the SPIRE maps to compute the column density map. This, in turn, has then been converted in an $A(\mathrm{V})$ map using the well-known relation $< [N(\mathrm{H}_1) + N(\mathrm{H}_2)]/E(\mathrm{B}-\mathrm{V}) >= 5.8 \times 10^{21}$ atoms cm^{-2} mag^{-1} (Bohlin et al. 1978). Finally, the mass enclosed within a certain $A(\mathrm{V})$ has been computed in the two cases: the Planck-based map and the AKARI-based one. The difference in percentage is reported in Table 4.

The difference is larger at small $A(\mathrm{V})$ because these regions corresponds to small column density and, in

[4]This statement is not meant to imply that the calibration made with Planck data is better than the one presented in this work.

turn, to small intensities of the dust emission. In these cases small variations of the offsets are more important. In any case, however, the difference is smaller than 10% even at $A(\mathrm{V})$ as low as 2 mag. We conclude that in terms of column density, the calibration made with AKARI gives the same, within the uncertainties, results obtained with the Planck calibration.

3.3 A mosaic of the Galactic plane

Work in progress.

4 Results and conclusions

In this report we have shown that it is possible to derive the zero-level of the diffuse emission of the PACS 160 μm band through a comparison with the AKARI WIDE-L band centred at 140 μm. We have analyzed only three cases (two in this version of the document), so that the statistics is not sufficient to make a conclusion on the general applicability of this method. Nonetheless, the three test cover different cases: a single map done with Scanamorphous and PACS calibration version 45 (corresponding to HIPE version 10); a mosaic of two maps generated with Unimap 6.2 and again calTree version 45; and, finally, a mosaic of three tiles of the Galactic plane with each map directly downloaded from the HSA, done with HIPE version 13.

In the first case, the Aquila region, the agreement is excellent with Planck and AKARI giving the same result. In the second case, the Perseus region, there is a difference betweent the offsets derived with Planck and AKARI, but on a global scale, considering the column density maps, the differences are well below the expected uncertainties.

Finally, for the Hi-Gal fields, ...

We conclude that the method can be used in general for PACS fields even if the user has to keep in mind always that the test covers a very very tiny fraction of the PACS maps available in the HSA. In particular, the presence of two peaks, which implies two possible offsets, in the Perseus case would require further investigation which, on the current time-scale of the PACS ICC, is not possible.

A Useful scripts

A.1 regToXY

This IDL procedure opens a ds9 region file written in image coordinates and returns the coordinates of the vertices of the polygon. The coordinates can be used with the IDL routine `polyFillV` to find the indices of a 2D array enclosed inside the polygon.

```
Pro regToXY,filename,xx,yy

; filename : name of the region file in physical coordinates

openR,1,filename
riga = ''
nome = 'polygon('
repeat readF,1,riga until(strpos(riga,nome) eq 0)
close,1

result = strsplit(strmid(riga,strlen(nome)),',',/extract)
quanti = n_elements(result)
xx = dblarr(quanti/2)
yy = xx
indice = 0
```

```
for index = 0,quanti/2-1 do begin
  xx[index] = result[indice]
  yy[index] = result[indice + 1]
  indice = indice + 2
endfor

return
end
```

A.2 modBB

This `python` module returns the blackbody intensity at the required wavelength for a given temperature. It is used in the script `cfrPACSAkari.py`.

```
# LL in micron
def modBB(LL,Temp):

    from java.lang.Math import PI
    from herschel.ia.numeric.toolbox.basic import EXP

    hcK = 1.4387752
    dhc2 = 3.74177118e-5/PI # erg/s*cm^2

    wave = LL*1e-4 # da micron a cm
    alpha = Temp*wave

    return dhc2/wave**5/(EXP(hcK/alpha)-1.) # erg/s/cm/cm^2/sr
```

A.3 cfrPACSAkari

This script makes the actual comparison between AKARI and PACS. It also requires the dust temperature map released by the Planck team. This script can not be written in a general form so the user has to customize it to her/his needs. Here we explain step by step the case of the Perseus region.

```
#the user has to import in HIPE the RSRF of the AKARI WIDE-L band.
#It is here assumed that two vectors have been created with these data:
#'wave' and 'RSRF'

#the PACS transmission system
calTree = getCalTree()
lambda_red = calTree.photometer.filterTransmission.red.getColumn(1).data
transm_red = calTree.photometer.filterTransmission.red.getColumn(0).data

llAbs = calTree.photometer.absorption.wavelength
aaAbs = calTree.photometer.absorption.transmission
interp = CubicSplineInterpolator(Double1d(llAbs),Double1d(aaAbs))

howManyLambda = lambda_red.size
minL = lambda_red.where(lambda_red > llAbs[0]).toInt1d()[0]
maxL = lambda_red.where(lambda_red < llAbs[llAbs.size-1]).toInt1d()[0]
```

```
if (maxL == 0): maxL = howManyLambda

absRed = interp(lambda_red[minL:maxL])*transm_red[minL:maxL]

#vector of temperatures: 5,6,... 50 K
Temperature = Double1d().range(46)+5

#factors to transport AKARI flux <-> PACS flux
#for a modified blackbody with exponent 2
diffXP = lambda_red[minL+1:maxL]-lambda_red[minL:maxL-1]
diffXA = wave[1:]-wave[0:99]
rapporti = Double1d(46)
index = 0
beta = 2.   # modify here the exponent according to your needs
lambdaRange = lambda_red[minL:maxL]
for T in Temperature:
    soloBB = (300./lambdaRange)**beta*modBB(lambdaRange,T)*absRed
    sumY = (soloBB[1:] + soloBB[0:maxL-minL-1])/2.
    flux = SUM(diffXP*sumY)
    resultP = flux/30.2*0.016**2
    soloBB = (300./wave)**beta*modBB(wave,T)*RSRF
    sumY = (soloBB[1:] + soloBB[0:99])/2.
    flux = SUM(diffXA*sumY)
    resultA = flux/51.9*0.014**2
    rapporti[index] = resultP/resultA
    index = index + 1
    print T,resultP/resultA

#note that the vector wave is in decreasing order so that the integral
#is negative. This is taken into account later

# una T per punto da Planck
interp = CubicSplineInterpolator(Temperature,rapporti)

#here is the part that the user must customize.
#the example here is the Perseus region observed in two successive epochs.
#to cover the region theee AKARI fields are used

#first we read the temperature map from Planck. These data are saved
#in the tPr SimpleImage

#then we read the first field (Perseus4 which covers the western part of Perseus)
#smoothed and regridded to each of the three AKARI fields
#the data are stored in the SimpleImage pac.
#AKARI data are read from each field, one by one, and stored in aka

#1) Perseus 4 and l55 field

#AKARI maps are in ecliptic coordinates.
from herschel.ia.dataset.image.wcs import CoordsTranslator
cambiaCoord = CoordsTranslator(wcsAkari,wcsPlanck)
```

```
#we count the number of AKARI intensities larger than 25 MJy/sr,
#and PACS data not equal to zero
off = Double1d(aka.image.where((aka.image > 25) & (pac.image != 0)).length())
indexOff = 0
for iX in range(wcsAkari.naxis1):
    for iY in range(wcsAkari.naxis2):
        if (aka.image[iX,iY] < 25): continue
        if (pac.image[iX,iY] == 0): continue
        raDec = cambiaCoord.translate(aka.getWcs().getWorldCoordinates(iX,iY))
        XX,YY = tPr.getWcs().getPixelCoordinates(raDec)
        tPlanck = tPr.getIntensityWorldCoordinates(raDec[0],raDec[1])
        rapporto = interp(tPlanck)
        valore = -aka.image[iX,iY]*rapporto - pac.image[iX,iY]
        off[indexOff] = valore
        indexOff = indexOff + 1

#2) Perseus 4 and l59 field

cambiaCoord = CoordsTranslator(wcsAkari,wcsPlanck)
offNew = Double1d(aka.image.where((aka.image > 25) & (pac.image != 0)).length())
indexOff = 0
for iX in range(wcsAkari.naxis1):
    for iY in range(wcsAkari.naxis2):
        if (aka.image[iX,iY] < 25): continue
        if (pac.image[iX,iY] == 0): continue
        raDec = cambiaCoord.translate(aka.getWcs().getWorldCoordinates(iX,iY))
        XX,YY = tPr.getWcs().getPixelCoordinates(raDec)
        tPlanck = tPr.getIntensityWorldCoordinates(raDec[0],raDec[1])
        rapporto = interp(tPlanck)
        valore = -aka.image[iX,iY]*rapporto - pac.image[iX,iY]
        offNew[indexOff] = valore
        indexOff = indexOff + 1
off.append(offNew)

#3) Perseus 4 and l60 field

cambiaCoord = CoordsTranslator(wcsAkari,wcsPlanck)
offNew = Double1d(aka.image.where((aka.image > 25) & (pac.image != 0)).length())
indexOff = 0
for iX in range(wcsAkari.naxis1):
    for iY in range(wcsAkari.naxis2):
        if (aka.image[iX,iY] < 25): continue
        if (pac.image[iX,iY] == 0): continue
        raDec = cambiaCoord.translate(aka.getWcs().getWorldCoordinates(iX,iY))
        XX,YY = tPr.getWcs().getPixelCoordinates(raDec)
        tPlanck = tPr.getIntensityWorldCoordinates(raDec[0],raDec[1])
        rapporto = interp(tPlanck)
        valore = -aka.image[iX,iY]*rapporto - pac.image[iX,iY]
        offNew[indexOff] = valore
        indexOff = indexOff + 1
```

```
off.append(offNew)

#Preparation of the histogram
from herschel.ia.numeric.toolbox.basic import Histogram
from herschel.ia.numeric.toolbox.basic import BinCentres

binSize = 1 # 1MJY/sr
hist = Histogram(binSize)
asseX = BinCentres(binSize)
p = PlotXY(asseX(off),hist(off))

#Looking for the maxima. For this example the first max is at 42.6 MJy/sr,
#the second at 53.6 MJy/sr
print hist(off).where(hist(off) == MAX(hist(off)))
print asseX(off)[1281],MAX(hist(off))
print hist(off)[1285:].where(hist(off)[1285:] == MAX(hist(off)[1285:]))
print asseX(off)[1285:][7],MAX(hist(off)[1285:])
print (42.5292279689+53.5292279689)/2

#Now we read the data of Perseus 2 (East Perseus)

#4) Perseus 2 and l59 field

cambiaCoord = CoordsTranslator(wcsAkari,wcsPlanck)
off2 = Double1d(aka.image.where((aka.image > 25) & (pac.image != 0)).length())
indexOff = 0
for iX in range(wcsAkari.naxis1):
    for iY in range(wcsAkari.naxis2):
        if (aka.image[iX,iY] < 25): continue
        if (pac.image[iX,iY] == 0): continue
        raDec = cambiaCoord.translate(aka.getWcs().getWorldCoordinates(iX,iY))
        XX,YY = tPr.getWcs().getPixelCoordinates(raDec)
        tPlanck = tPr.getIntensityWorldCoordinates(raDec[0],raDec[1])
        rapporto = interp(tPlanck)
        off2[indexOff] = -aka.image[iX,iY]*rapporto - pac.image[iX,iY]
        indexOff = indexOff + 1

#5) Perseus 2 and l60 field

offNew = Double1d(aka.image.where((aka.image > 25) & (pac.image != 0)).length())
indexOff = 0
for iX in range(wcsAkari.naxis1):
    for iY in range(wcsAkari.naxis2):
        if (aka.image[iX,iY] < 25): continue
        if (pac.image[iX,iY] == 0): continue
        raDec = cambiaCoord.translate(aka.getWcs().getWorldCoordinates(iX,iY))
        XX,YY = tPr.getWcs().getPixelCoordinates(raDec)
        tPlanck = tPr.getIntensityWorldCoordinates(raDec[0],raDec[1])
        rapporto = interp(tPlanck)
        offNew[indexOff] = -aka.image[iX,iY]*rapporto - pac.image[iX,iY]
        indexOff = indexOff + 1
```

```
off2.append(offNew)
p = PlotXY(asseX(off2),hist(off2))
print hist(off2).where(hist(off2) == MAX(hist(off2)))
print asseX(off2)[318],MAX(hist(off2))
print hist(off2)[324:].where(hist(off2)[324:] == MAX(hist(off2)[324:]))
print asseX(off2)[324:][6],MAX(hist(off2)[324:])
print (54.6402921265+66.6402921265)/2
```

References

[1] Balog Z. et al., 2014, Exp. Astr., 37, 129

[2] Bernard J.-Ph. et al., 2010, A&A, 518, L88

[3] Bohlin R.C., Savage B.D. & Drake J.F., 1978, ApJ, 224, 132

[4] Kawada M. et al., 2007, PASJ, 59, 389

[5] Könyves V. et al., 2015, A&A, 584, 91K

[6] Pezzuto S. et al., 2012, A&A, 547, A54

[7] Pezzuto S., 2013, PICC-CR-TN-044 (http://herschel.esac.esa.int/twiki/pub/Public/PacsCalibrationWeb/PICC-CR-TN-044.pdf

[8] Planck results 2013. XI, 2014, A&A, 571, A11

[9] Piazzo L. et al., 2015, MNRAS, 447, 1471

[10] Sadavoy S.I. et al., 2013, ApJ, 767, 126

[11] Takita S. et al., 2015, PASJ, 67, 51 (AkaPaper)